Supporting Information

Prusinkiewicz et al. 10.1073/pnas.0906696106

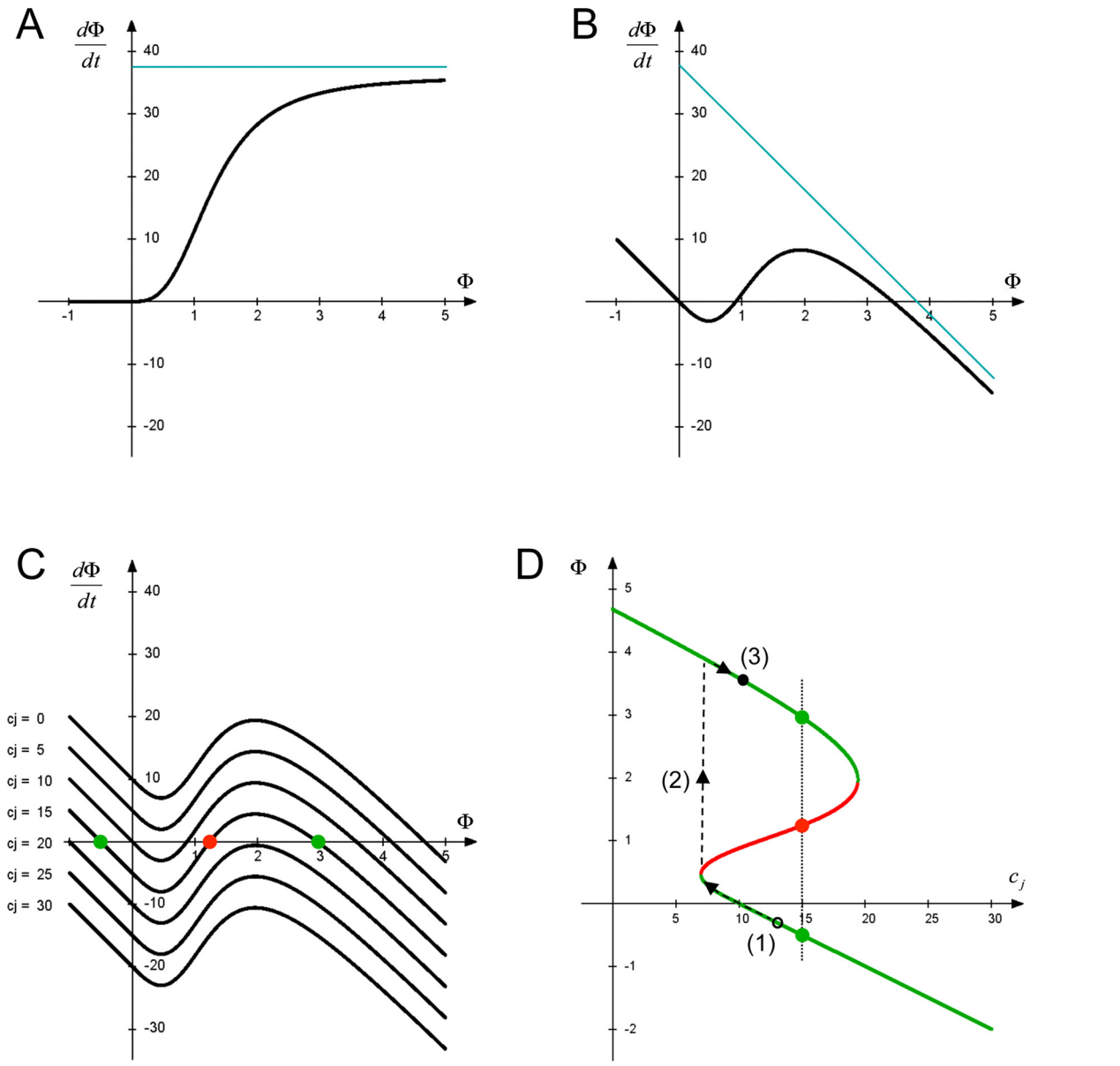

Fig. S1. Qualitative analysis of the dynamical system described by Eq. **8**. Parameter values are given in Table S1; all plots have been drawn assuming source auxin concentration $c_j = 10$. (*A*–*C*) Graphical interpretation of the Eq. **8**. (*A*) A sigmoidal curve described by the term $\rho T c_i \Phi^n/(K^n + \Phi^n)$ for $\Phi \geq 0$ and 0 for $\Phi < 0$. (*B*) The sheared curve obtained by subtracting the term $\mu\Phi$ from the term depicted in (*A*). The blue lines in (A) and (*B*) are the asymptotes for $\Phi \to \infty$. (*C*) The family of curves resulting from the addition of the term $(\mu D + \rho_0 T)(c_i - c_j)$, for different auxin concentrations in the sink c_j, to the curve (*B*). Green dots show stable equilibria, and the red dot shows the unstable equilibrium for the sample concentration $c_j = 15$. (*D*) Bifurcation diagram, showing positions of equilibria as a function of sink concentration c_j. Green and red dots indicate these equilibria for the concentration $c_j = 15$, corresponding to (*C*). The entire diagram (hysteresis curve) was obtained by plotting positions of stable and unstable equilibria for values c_j ranging from 0 to 30. Black arrows and dashed lines indicate a sample progression of states of a face between a source and a sink, which occurs when the sink auxin concentration c_j first decreases, then increases: flux Φ jumps (line 2) from the initial small value (open black circle 1) to the large final value (closed black circle 3). This progression is at the heart of the switch of the lateral bud from the dormant to active state, *cf.* Fig. S2 *B*–*D*.

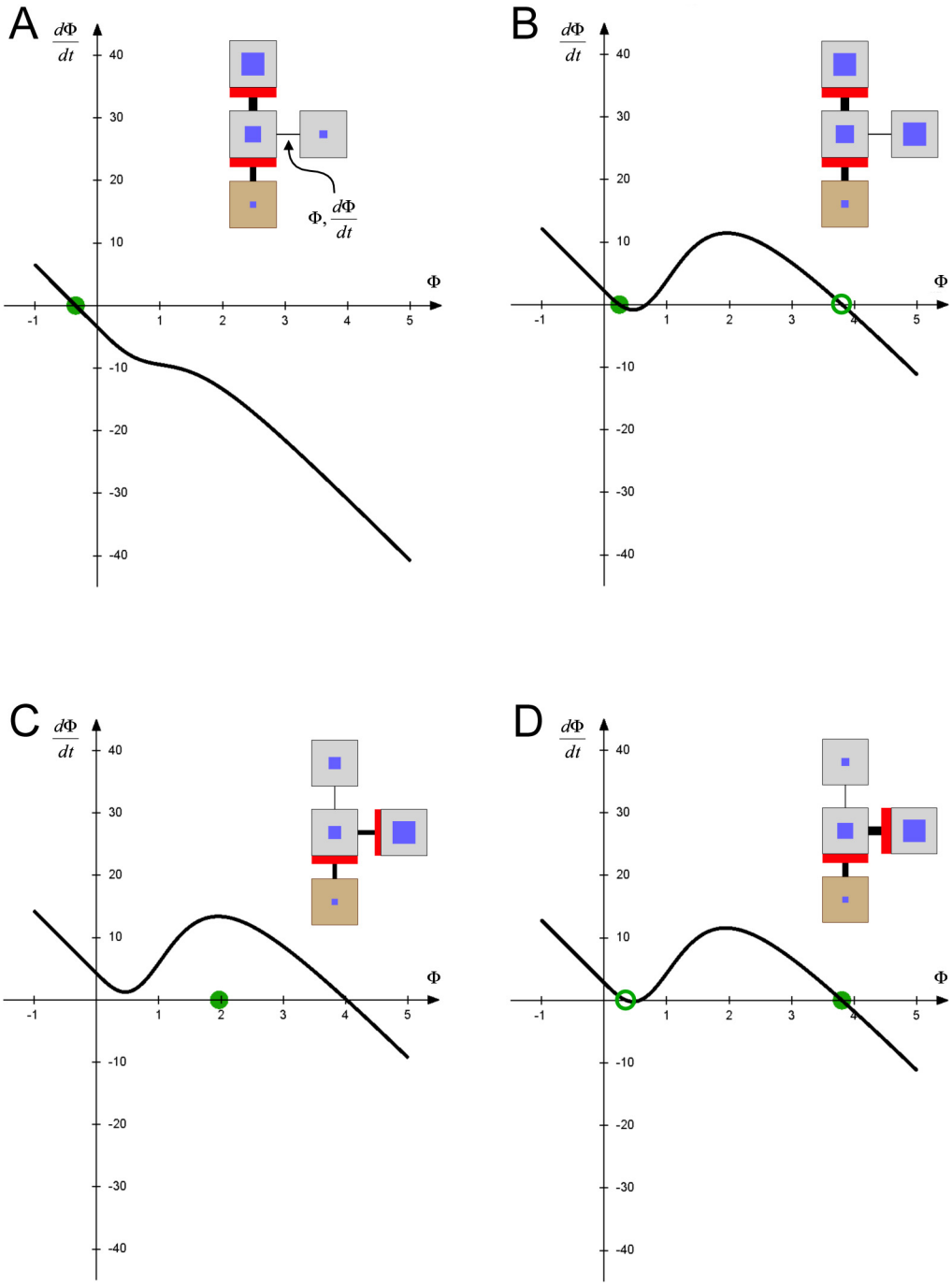

Fig. S2. Typical progression of patterns of auxin transport in a branching structure from Fig. 1, simulated using a canalization model (Eqs. **1**, **2**, and 10). The modeled structure (*Inset*) is the same as in Fig. 1. Plots associated with each structure show the rate of change of auxin efflux from the lateral bud, $d\Phi/dt$, as a function of the efflux Φ from this bud (Eqs. **8a** and **b**). The filled green circle indicates current flux Φ. The simulation was driven by a user, who interactively increased auxin production in the lateral bud between stages A and B, then decreased auxin production in the terminal metamer between stages B and C. (*A*) The initial state: auxin originating in the terminal metamer is transported through the branching node to the sink. There is a small negative flux from the branching node to the lateral bud due to diffusion and/or residual amounts of PIN proteins present in all faces. (*B*) Local auxin production has been increased, augmenting auxin concentration in the bud. A second stable state emerges (open green circle), but auxin efflux from the bud remains low due to the continuous progression from state A to B. (*C*) Auxin production in the terminal metamer has been decreased, leading to reduced auxin concentration in the branching node. The function plot shifts upward, making the previous stable state disappear. As a result, flux Φ jumps toward the remaining stable state, characterized by high auxin efflux from the lateral bud. (*D*) Auxin supply from the lateral bud increases auxin concentration in the branching node. The first stable state reappears (open green circle), but efflux from the lateral bud remains high. The path of auxin influx into the branching node has thus switched from the terminal to the lateral metamer, reflecting the history of the system. The progression of states depicted in Figs. *B* to *D* corresponds to the progression of states (1)-(3) in Fig. S1*D*.

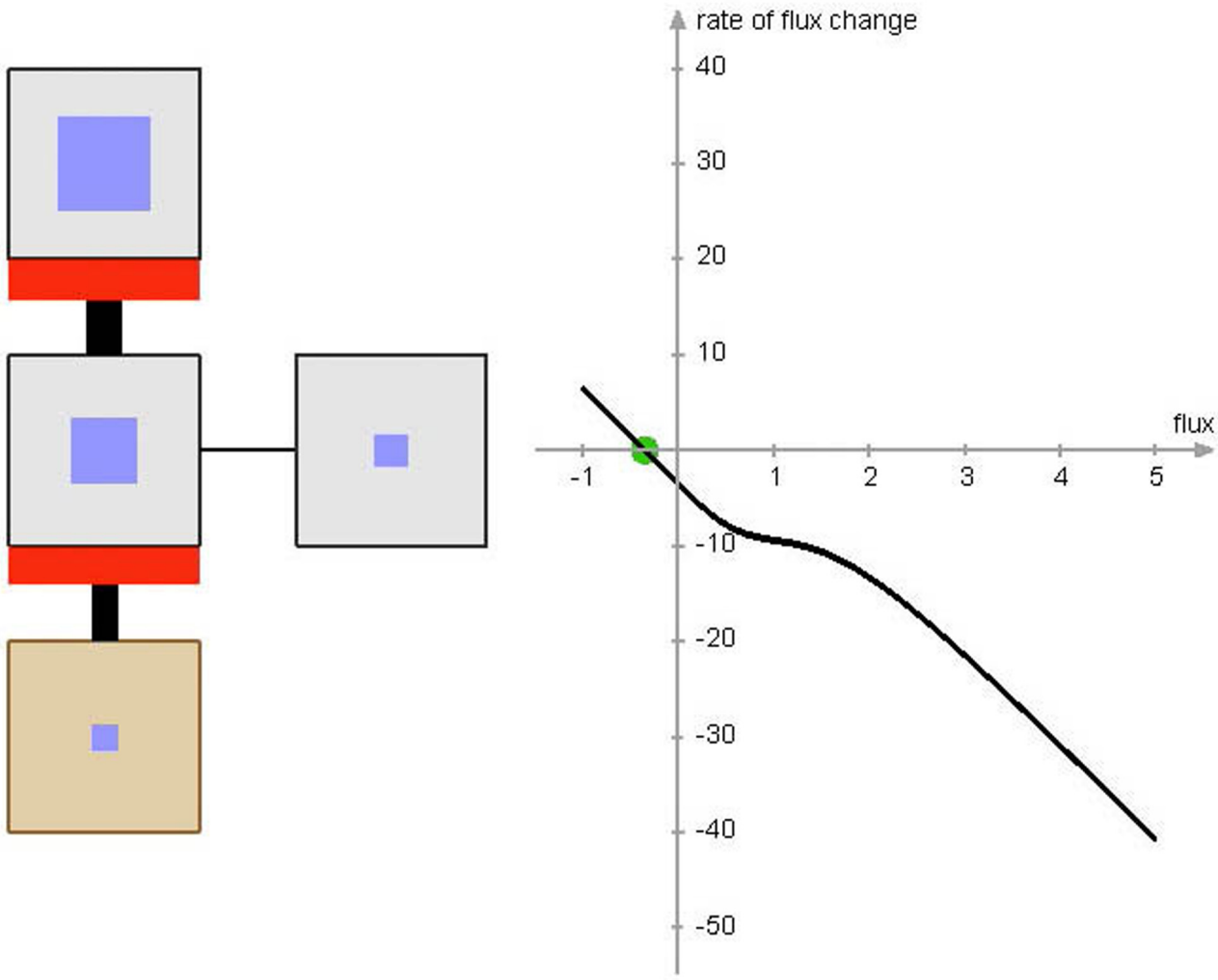

Movie S1. Typical progression of auxin transport at a branching node. Simulation was controlled interactively, by first increasing auxin production in the lateral bud, then decreasing production in the terminal bud. The dynamic plot characterizes auxin efflux from the lateral bud.

Movie S1 (MOV)

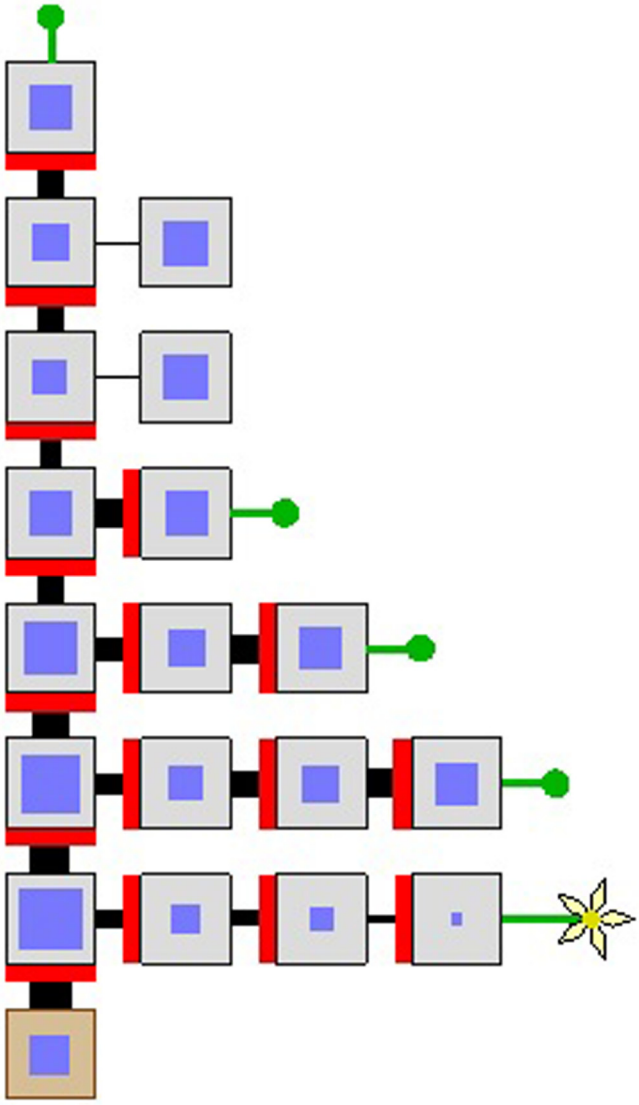

Movie S2. Simulation of a decapitation experiment in the *axr3* mutant. Removal of the shoot apical meristem activates the lateral bud immediately below the decapitation site.

Movie S2 (MOV)

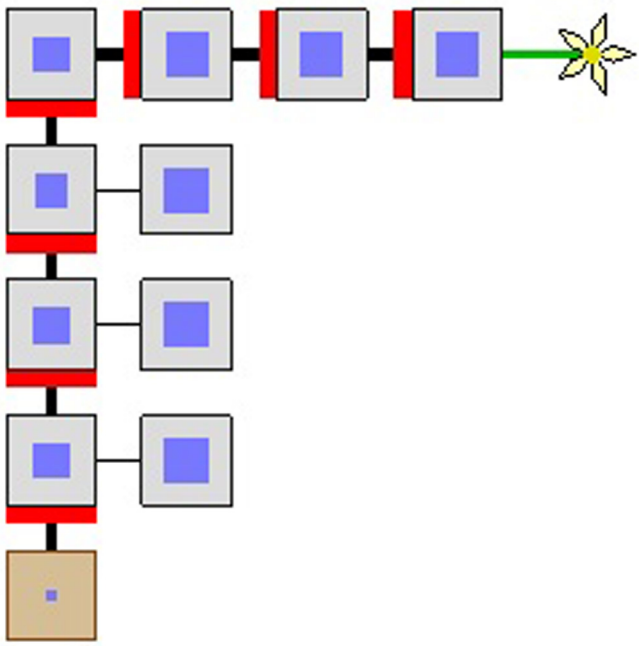

Movie S3. Simulation of a decapitation experiment in the *axr3* mutant. Removal of the shoot apical meristem activates the lateral bud immediately below the decapitation site.

Movie S3 (MOV)

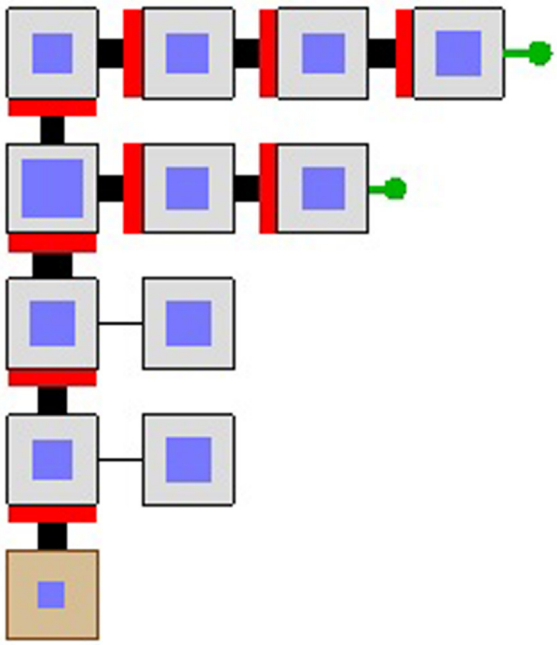

Movie S4. Simulation of a decapitation experiment with overcompensation. Removal of the shoot apical meristem activates the 2 lateral buds closest to the decapitation site.

Movie S4 (MOV)

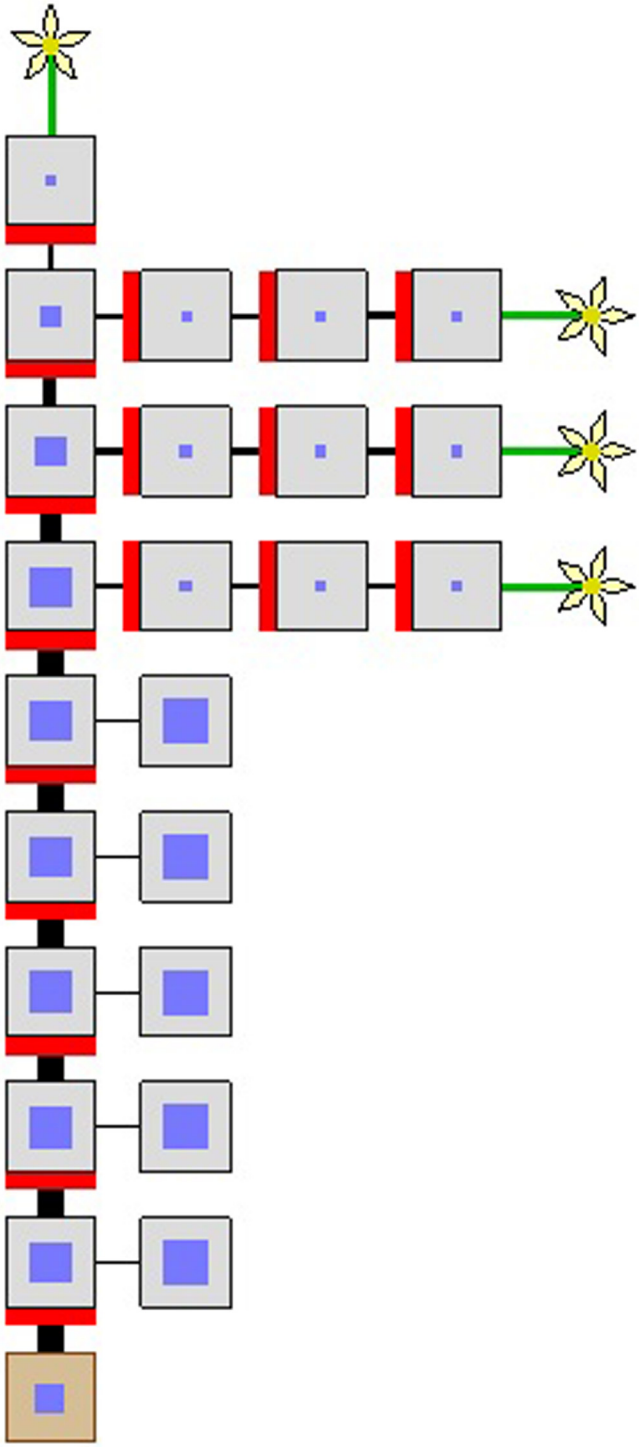

Movie S5. Basipetal propagation of bud activation as found in WT Arabidopsis. The cascade of bud activation stops at 3 lateral buds due to residual auxin production after floral transition.

Movie S5 (MOV)

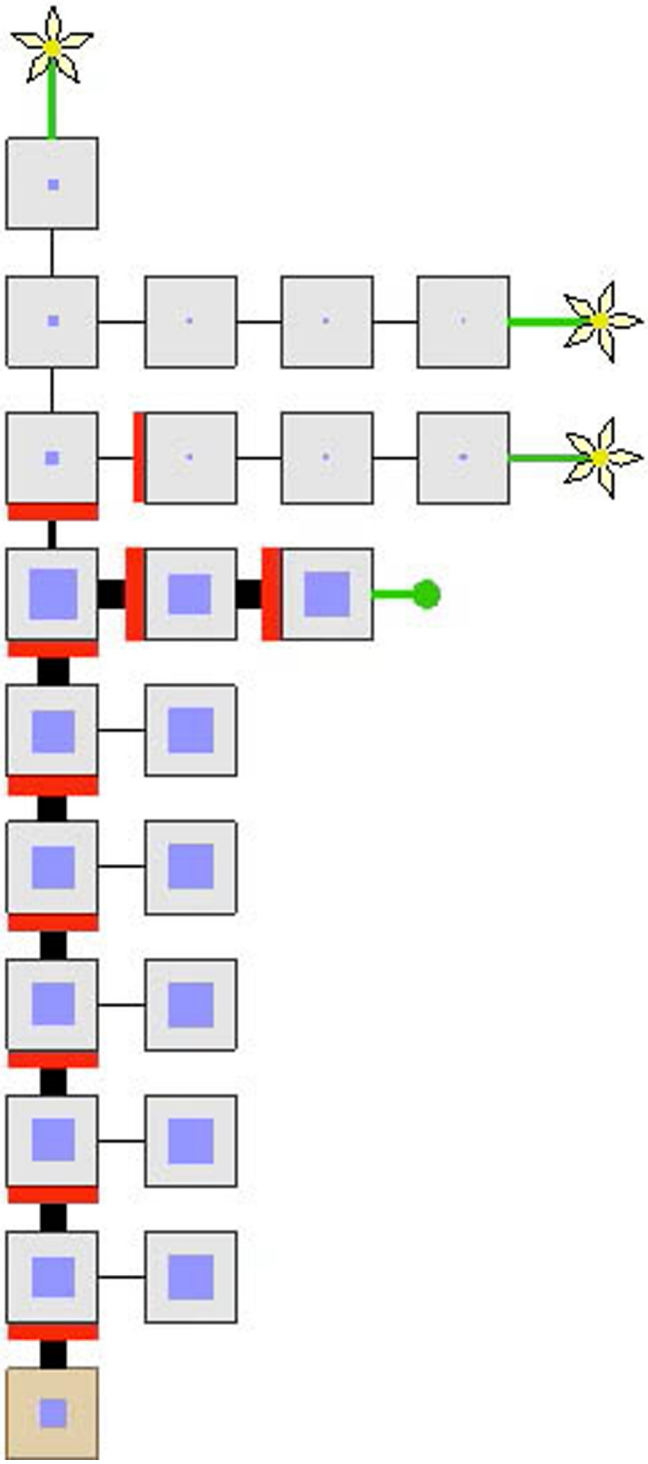

Movie S6. Unlimited basipetal propagation of bud activation. Simulation parameters are the same as in Animation S5 except for the residual auxin production, which is set to 0.

Movie S6 (MOV)

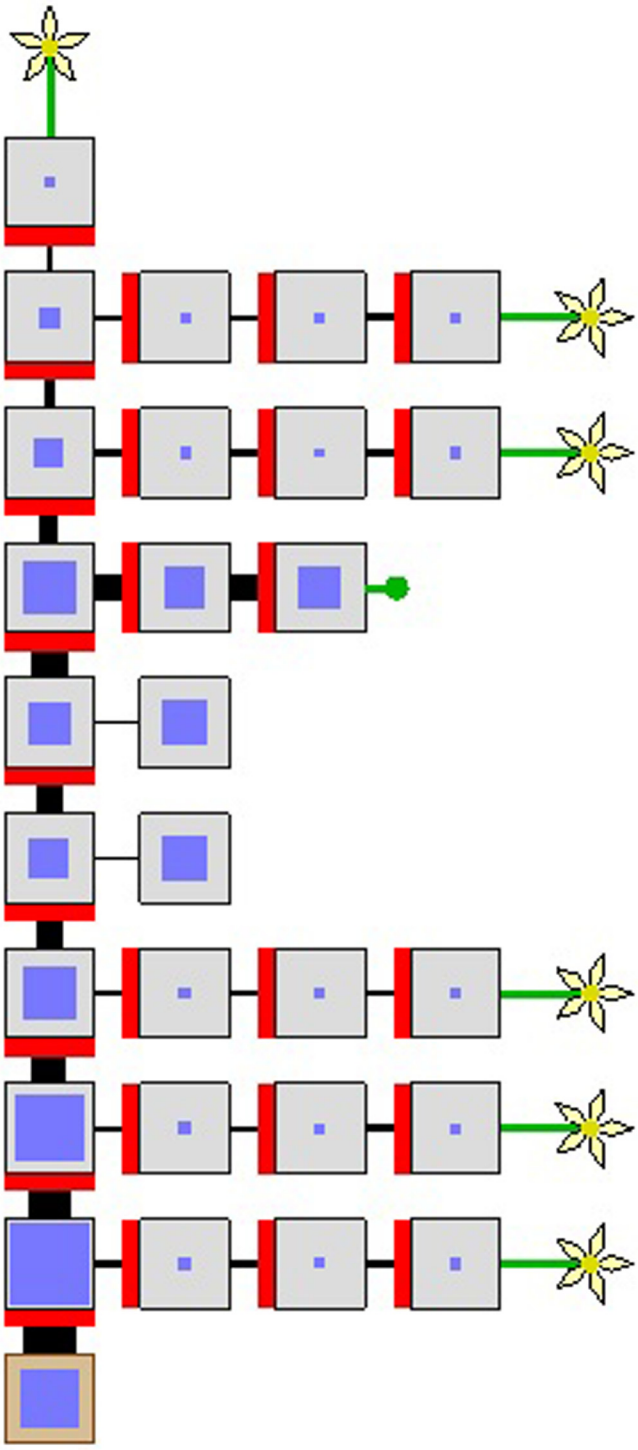

Movie S7. Simulation of a convergent activation pattern.

Movie S7 (MOV)

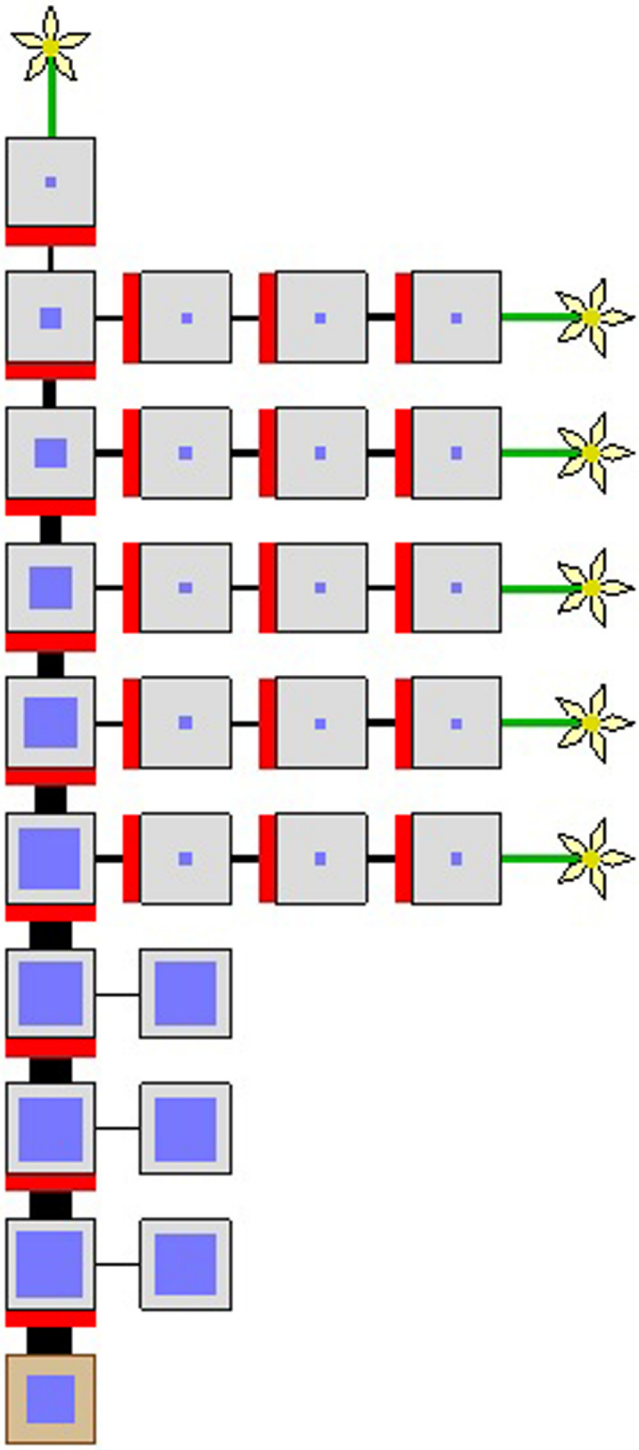

Movie S8. Simulation of bud activation in the *axr1* mutant.

Movie S8 (MOV)

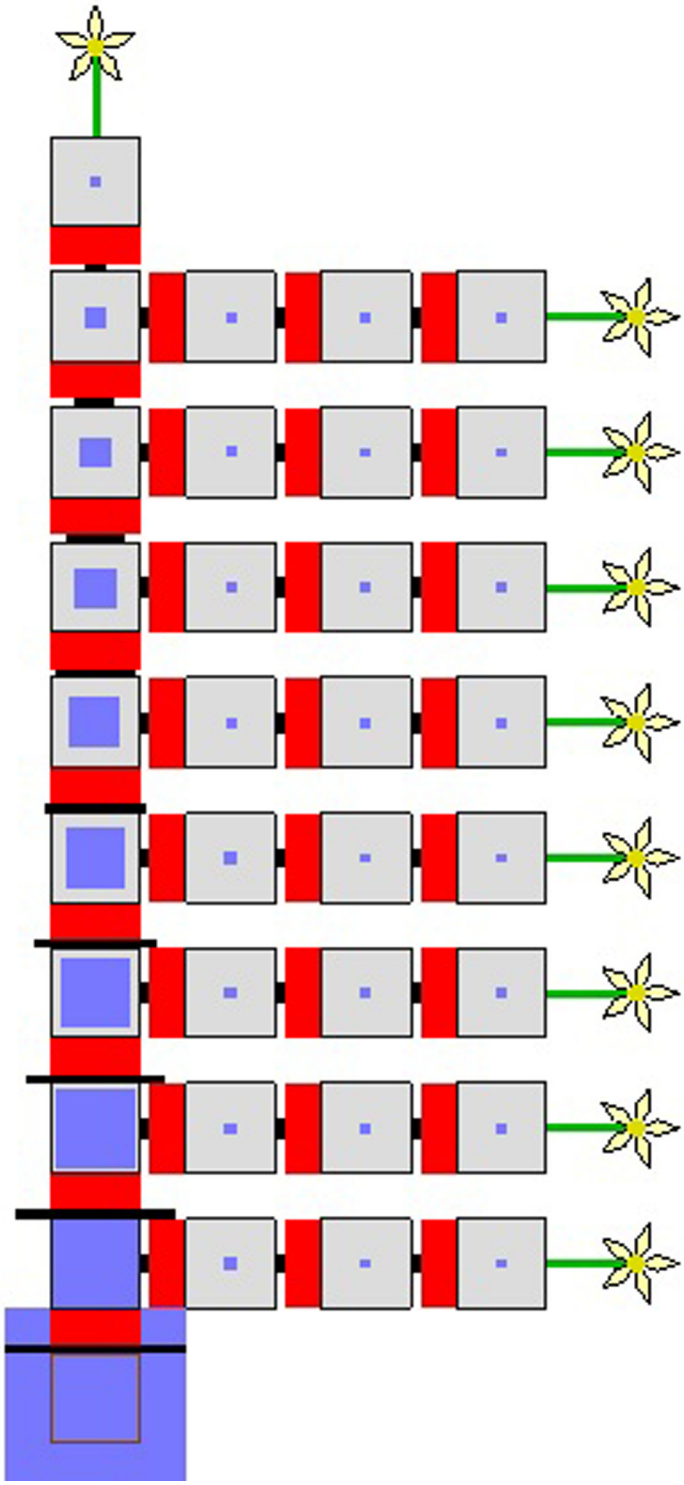

Movie S9. Simulation of bud activation in the *max4* mutant.

Movie S9 (MOV)

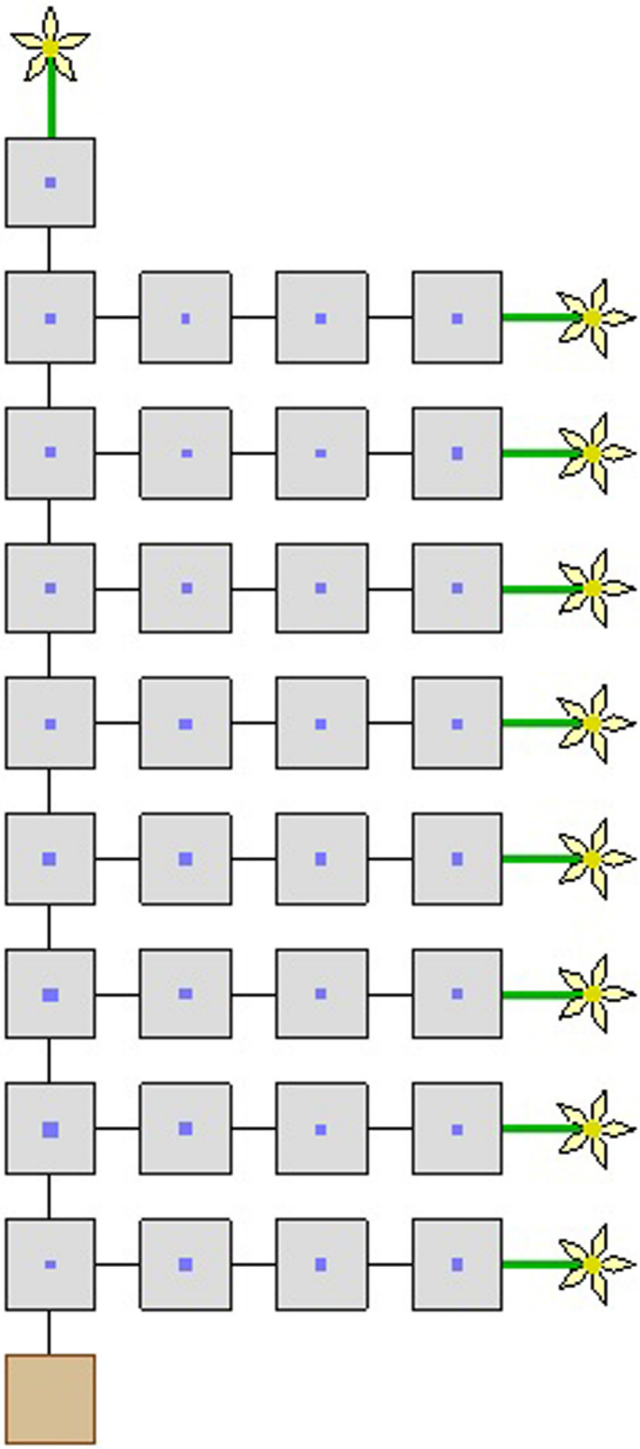

Movie S10. Simulation of bud activation in the *tir3* mutant.

Movie S10 (MOV)

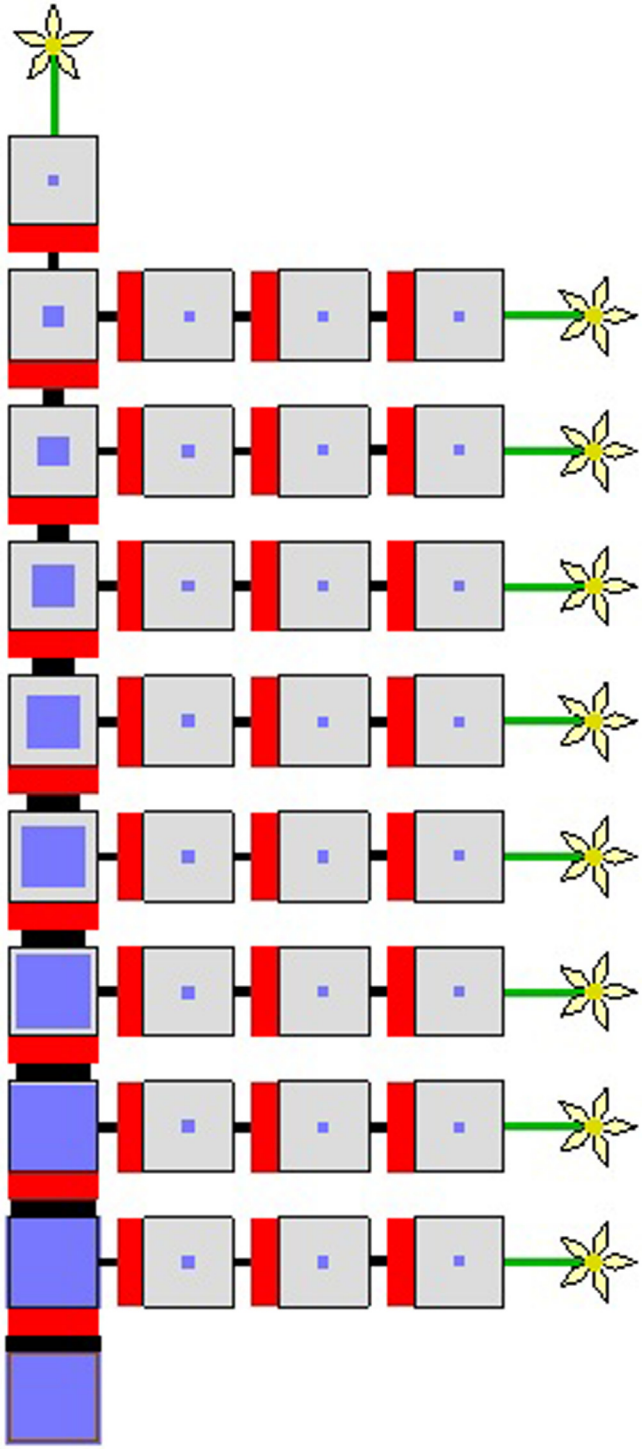

Movie S11. Simulation of bud activation in the double *max4,tir3* mutant.

Movie S11 (MOV)

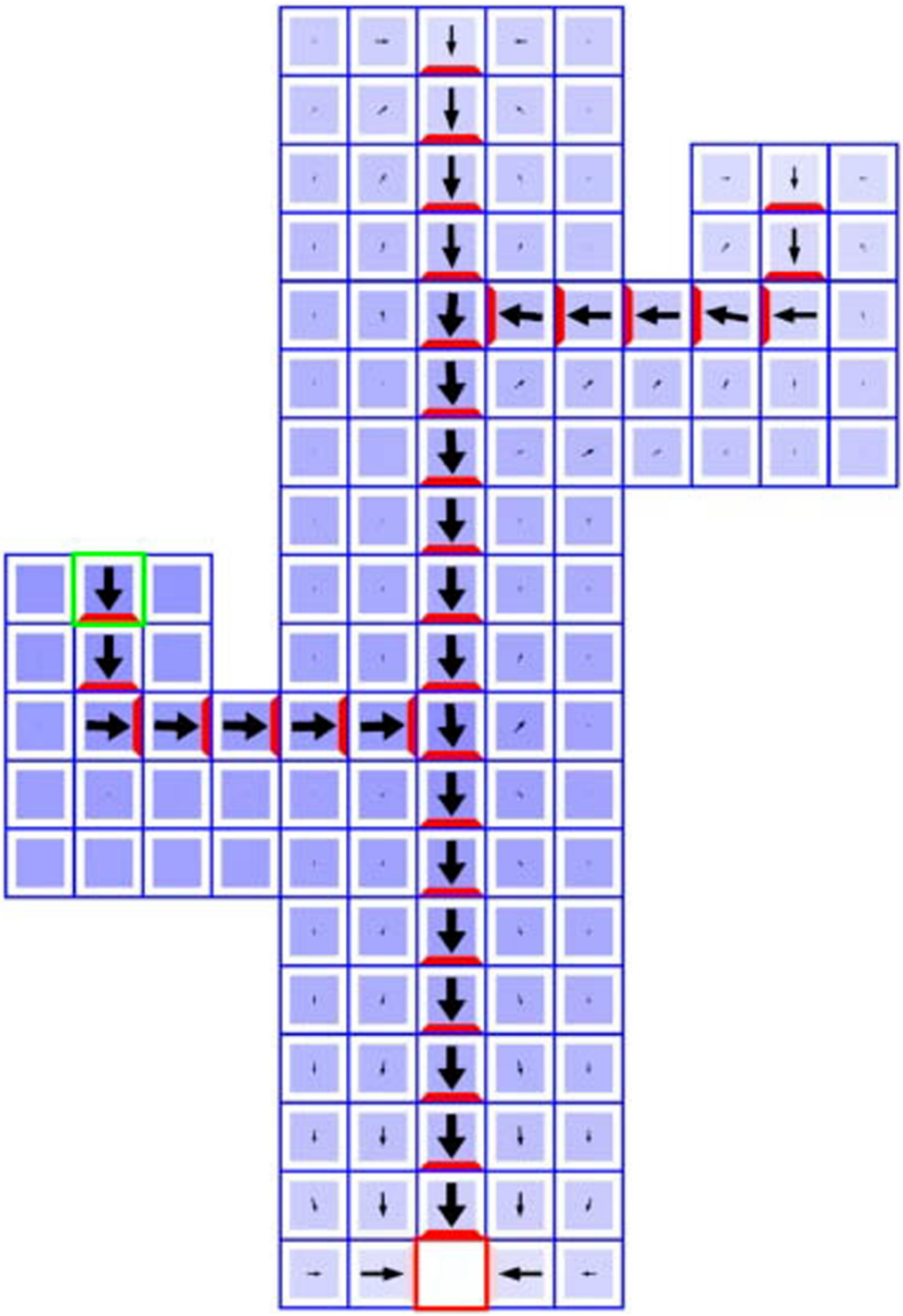

Movie S12. Simulation of bud activation at the cellular level.

Movie S12 (MOV)

Table S1. Parameter values used in simulations. Simulations are divided into 3 groups. Within each group, all simulations use the same parameter values except when shown otherwise

Parameter		Simulation group 1			2									3
Name	Symbol	S1A	S1 B-D	S2, 1B-F	2D-F acropetal	2G-H *axr3*, repl.	2I overcomp.	3A-E w.t.	3F converg.	4A *axr1*	5D *max4*	5E *tir3*	5F *max4,tir3*	5B-F cell-level
Polar transport coefficient	T	0.5				0.2		0.5						2
Diffusion coefficient	D	0.1						0.02						2
PIN allocation rate	$\rho_{i\to j}$	7.5						10				5	5	0.17
Hill exponent	n	3						3						3
Hill saturation coefficient	K	1.3						0.5						10
Base PIN production rate	ρ_0	0						0.15						0.15
PIN turnover rate	μ	0	10	10				7.5			2.5		2.5	0.1*
Target auxin concentration	H	N/A		10				10		14				10
Residual auxin concentration	H_r	N/A		3.0		10	10	2.5						10
Auxin production rate	σ	N/A		10				10						10
Residual auxin production rate	σ_r	N/A		10				10						0.08
Auxin turnover rate	ν	N/A		0.1	0.2			0.005	0.03					0.08
Auxin turnover in the root	ν_{root}	N/A		1.0				1.0						N/A†
Metamer/cell volume	V_i	N/A		1.0				1.0						1.0
Face area	$A_{i,j}$	N/A		1.0				1.0						1.0
Threshold bud-activation flux	Φ_{th}	N/A						2.0						N/A
Simulation time step	Δt	N/A		0.05				0.05						0.05
Frames shown		N/A	N/A	‡	0, 50, 130	175, 275§	238§	0, 70, 225, 400, 1500	485	2000	2000¶	2000	2000	450, 6750, 13500, 22500, 38250

*After reaching the value of 1.0, surface PIN concentration cannot drop below 1.0.
†Auxin concentration in the basal cell is fixed at 0.
‡Simulation controlled interactively.
§Plant decapitated interactively after simulation step 175
¶PIN concentration visualized at a scale reduced by 1/3 w.r.t. the other simulations.

Other Supporting Information Files

SI Appendix (PDF)